Plasmonic modes in a dispersive left handed material optical fiber

A. Mendoza-Suárez
Facultad de Ciencias Físico-Matemáticas, Universidad Michoacana de San Nicolás de Hidalgo,
Edificio "B", Ciudad Universitaria 58060, Morelia, Michoacán, México,
e-mail: almend@zeus.umich.mx

F. Villa-Villa
Centro de Investigaciones en Óptica,
Lomas del Bosque 115, Lomas del Campestre, León, Gto. 37150, México,
e-mail: fvilla@cio.mx

J.A. Gaspar-Armenta
Centro de Investigación en Física de la Universidad de Sonora,
Apdo. Postal 5-088, Hermosillo Sonora 83190, México,
e-mail: jgaspar@cajeme.cifus.uson.mx

Recibido el 9 de mayo de 2008; aceptado el 12 de junio de 2008

We determine the presence of plasmonic surface modes under TE polarization in an optical fiber made of a dispersive left handed material. These modes keep clearly localized at a constant frequency within the numerical error, despite strong geometrical changes in the physical system. To prove this fact we analyze systems having random roughness on their surfaces and consider other geometry variations. The electromagnetic field distribution is determined in the region where plasmonic and non plasmonic modes exist.

Keywords: Optical fiber; surface modes; left handed material.

Determinamos la presencia de modos de superficie plasmónicos para polarización TE en una fibra óptica hecha de un metamaterial izquierdo. Estos modos se mantienen claramente localizados a una frecuencia constante dentro del error numérico de la simulación a pesar de que el sistema físico se somete a grandes cambios en su geometría. Para probar este hecho, analizamos sistemas que poseen rugosidad aleatoria en sus superficies y consideramos otras variaciones en la geometría. Determinamos en la región in la región del espectro donde existen modos plasmónicos y no plasmónicos.

Descriptores: Fibra óptica; modos de superficie; metamateriales.

PACS: 41.20.5b; 42.81.-I; 42.82.Et

1. Introduction

Structured materials that have recently attracted much interest are the left handed materials (LHM) which owe their name to the fact that the light vectors $\vec{E}$, $\vec{H}$ and $\vec{k}$ form a left handed triad for a wave propagating through these media. LHM are periodic arrays of metallic entities in vacuum with a unit cell of dimensions much smaller than the wavelength [1]. Although fundamental experiments with LHM have been developed for the microwave region of the electromagnetic spectrum, there exist recent results indicating that LHM are now available at visible and infrared regions [2-3].

Since these materials have a negative refractive index within a given range of the electromagnetic spectrum, some of the well known optical phenomena present variations that make them potentially useful for new technological applications like for example negative refraction. As a consequence the scientific community has started to study a variety of optical systems that include LHM as regular components.

The case of optical fibers is not the exception and some studies have been proposed to analyze the scattering properties of infinitely long cylinders made of left handed materials [4-5].

In this work, we analyze the existence of plasmonic surface modes that appear at the surface of an optical fiber made of LHM by using an integral method to solve the Helmholtz equation. Most of the numerical methods used to simulate the propagation of light in optical systems consider only smooth surfaces. However, real devices involve surfaces that present some roughness. Such roughness is random in nature and in certain situations this roughness can be neglected but in others do not. It is well known that the random roughness present in real systems can produce interesting phenomena like the enhanced backscattering [6-7]. So, we will consider that the surface of the optical fiber has some roughness or some other geometry variations.

2. Theory

Assuming a sinusoidal time dependence $e^{-i\omega t}$ for the electromagnetic fields, the wave equation can be transformed to the Helmholtz equation

$$\nabla^2 \Psi_j(\vec{r}) + k_j^2 \Psi_j(\vec{r}) = 0. \quad (1)$$

In this equation $\Psi_j(\vec{r})$ represents the electric field E_z in the case of TE-polarization in the jth medium (Fig. 1). The

magnitude of the wave vector is given by

$$k_j = n_j(\omega)\frac{\omega}{c}, \tag{2}$$

where the refractive index $n_j(\omega) = \pm\sqrt{\mu_j(\omega)\varepsilon_j(\omega)}$ that involves the material's properties is given in terms of the magnetic permeability $\mu_j(\omega)$ and the electric permitivity is given by $\varepsilon_j(\omega)$ both of these functions depending on the frequency ω. The speed of light is indicated by c. The sign appearing in the refractive index equation must be taken negative when considering a LHM and positive when the medium is a dielectric material.

The optical properties of LHM are given by the dielectric function

$$\varepsilon(\omega) = 1 - \left(\frac{\omega_p}{\omega}\right)^2, \tag{3}$$

and the magnetic permeability function

$$\mu(\omega) = 1 - \frac{F}{1-(\omega_0/\omega)^2}. \tag{4}$$

In these expressions ω_p=$10c/D$, ω_0=$4c/D$, F=0.56. D is a normalization constant that we choose to be the dimension of the side of the perfect conductor square (Fig. 1). We will be using also a normalized frequency given by $\bar{\omega}$=$\omega D/2\pi c$.

For a flat surface LHM-vacuum, there exist a plasmonic surface mode when $k_{||} \to \infty$ (the parallel component of the wave vector goes to infinity) when $\mu(\omega_{psw}) = -1$, being $\bar{\omega}_{psw} = \bar{\omega}_0\sqrt{2/(2-F)} = 0.752$ [4].

Let us consider an optical fiber composed of a LHM in vacuum and enclosed within a perfect conductor cavity as shown in Fig. 1. The Γ_2 profile is a square, while the Γ_1 corresponds to the profile of the transverse section of the optical fiber. The reason to use a perfect conductor is to keep a simple model of the optical fiber.

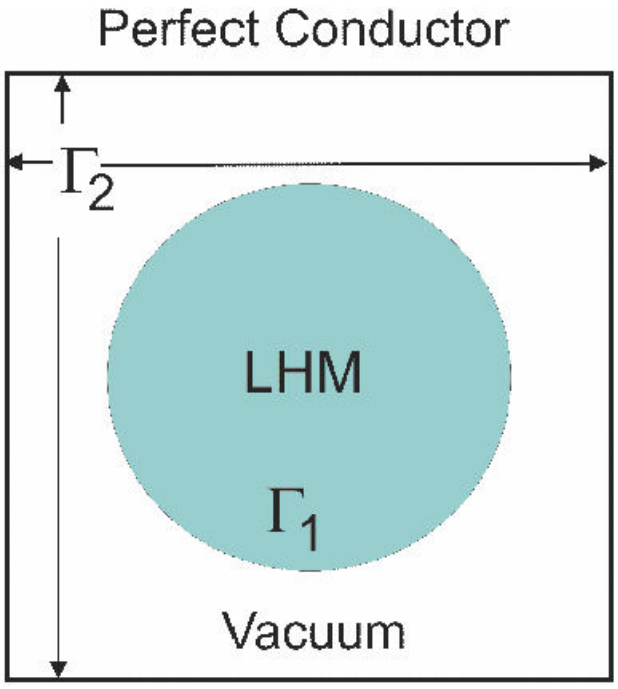

FIGURE 1. Transverse section of an optical fiber enclosed in a square cylinder cavity of a perfect conductor.

By applying the two-dimensional Green's second integral theorem to $\Psi_j(\vec{r}\,')$ for each region corresponding to the j-th medium, we have [6-7]

$$\oint_{C_j}\left[G_j(\vec{r},\vec{r}\,')\frac{\partial\Psi_j(\vec{r}\,')}{\partial n_j'} - \frac{\partial G_j(\vec{r},\vec{r}\,')}{\partial n_j'}\Psi_j(\vec{r}\,')\right]ds' = 0, \tag{5}$$

where $G_j(\vec{r},\ \vec{r}\,')$ is a usual Green function [6,7]. The sources $\Psi_j(\vec{r},\ \vec{r}\,')$ and $\partial\Psi_j(\vec{r}\,')/\partial n_j'$ involved in Eq. (5) can be determined numerically by transforming it to an homogeneous system of equations $M(\omega)F(\omega) = 0$, where the function $F(\omega)$ is a column matrix that contains the sources. For our system, the matrix $M(\omega)$ can be expressed as

$$M(\omega) = \begin{pmatrix} -L^{(1)}_{mn\,(11)} & N^{(1)}_{mn\,(12)} & -L^{(1)}_{mn\,(12)} \\ -L^{(1)}_{mn\,(21)} & N^{(1)}_{mn\,(22)} & -L^{(1)}_{mn\,(22)} \\ 0 & N^{(2)}_{mn\,(22)} - \delta_{mn\,(22)} & -\mu L^{(2)}_{mn\,(22)} \end{pmatrix}. \tag{6}$$

The matrix elements are given by

$$L^{(p)}_{mn\,(ij)} = \frac{i\Delta s}{4}H_0^{(1)}\left(k_p d_{mn(ij)}\right)\left(1-\delta_{mn(ij)}\right) + \frac{i\Delta s}{4}H_0^{(1)}\left(k_p\frac{\Delta s}{2e}\right)\delta_{mn(ij)}, \tag{7}$$

$$N^{(p)}_{mn\,(ij)} = \frac{i\Delta s}{4}k_p H_1^{(1)}\left(k_p d_{mn(ij)}\right)\frac{D_{mn}}{d_{mn\,ij}}\left(1-\delta_{mn\,(ij)}\right) + \left(\frac{1}{2}+\frac{\Delta s}{4\pi}D'_{n\,(ij)}\right)\delta_{mn(ij)}, \tag{8}$$

with

$$d_{mn(ij)} = \sqrt{\left(X_{m\,(i)} - X_{n\,(j)}\right)^2 + \left(Y_{m\,(i)} - Y_{n\,(j)}\right)^2}, \tag{9}$$

$$D_{mn\,(ij)} = -Y'_{n\,(j)}\left(X_{m\,(i)} - X_{n\,(j)}\right) + X'_{n\,(j)}\left(Y_{m\,(i)} - Y_{n\,(j)}\right), \tag{10}$$

$$D'_{n\,(ij)} = X'_{n\,(i)}Y''_{n\,(j)} - X''_{n\,(i)}Y'_{n\,(j)}. \tag{11}$$

In the previous expressions, $H_i^{(1)}(z)$ is the Hankel's function of first class and order i.The symbol $\delta_{mn\,(ij)}$ stands for a Kronecker's delta, with $mn\,(ij)$ meaning the mth point along the Γ_i and the nth contour Γ_j, with $i, j = 1, 2$. The Δs parameter is the arc length between two consecutive points $\left(X_{n\,(i)},\ Y_{n\,(i)}\right)$. Finally, $k_p = n_p\omega/c$, with $p = 1,\ 2$, corresponding to vacuum or the LHM, respectively.

To determine the frequency ω_j, we define the real function

$$D_t(\omega) = \ln\left(\left|Det\ (M)\ \right|\right), \tag{12}$$

whose relative minima can be identified as the frequency of the modes.

Given the mode frequency ω_j we can use the well known numerical method of single value decomposition [8] to obtain the non trivial solutions for $F(\omega_j)$ and the corresponding field.

3. Generating a random rough profile corresponding to a transverse section of a closed surface

We modeled the surface of an optical fiber by means of a numerically generated random roughness [9-10].

If the radial function $r{=}r(\theta)$, with $0{\leq}\theta{<}2\pi$, represents the required profile, let us consider the case where the average profile is a circumference of radius R, mathematically $\langle r(\theta)\rangle = R$.

We define a function

$$\delta r(\theta) = r(\theta) - R, \tag{13}$$

where $\delta r(\theta)$ represents the variation of a radial profile with reference to a circle of radius R. The random surface can be modeled by considering a Gaussian distribution given by

$$f(\delta r) = \left(1/\sqrt{2\pi\sigma}\right)\exp\left(-\frac{(\delta r)^2}{2\sigma^2}\right), \tag{14}$$

where σ represents the standard deviation of radius due to the surface.

Defining the angular correlation function by

$$B(\theta, \theta') = \exp\left(-\frac{(\theta - \theta')^2}{\Theta^2}\right), \tag{15}$$

where Θ stands for the "angular correlation length", and represents the angular scale of the random roughness. Assuming

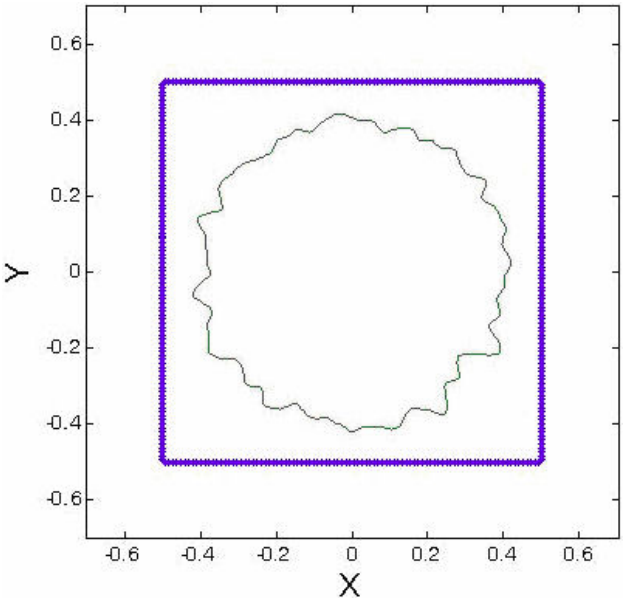

FIGURE 2. Scheme of the nucleus of a fiber when the surface is a realization of an ensamble with random roughness.

that the variation δr can be determined by using the linear relation

$$\delta r(\theta_k) = \sigma \sum_{j=-\infty}^{\infty} A_j X_{j+k}, \tag{16}$$

where A_j are the coefficients to be determined, and X_j constitutes a set of N independent Gaussian variables with zero media and standard radial deviation equal to one. We can show that

$$A_j = \left(\frac{2\Delta\theta}{\Theta\sqrt{\pi}}\right)^{1/2}\exp\left(-\frac{2(\Delta\theta)^2 j^2}{\Theta^2}\right). \tag{17}$$

With these tools we are able to numerically simulate profiles with a given random roughness. A typical example is shown in Fig. 2.

4. Numerical results

Let us consider an optical fiber enclosed in a square cylinder cavity, as mentioned before, whose transverse section has the filling fraction 0.5 (Fig.1). If we determine the modes by the method described in section 2, the plasmonic modes (extreme of the curves) [11-12] become evident when simulating with smooth surfaces (Fig. 3, left side) or adding roughness to the surface of the fiber (Fig. 3, right side). The parameters used to model the roughness were $\sigma = R/25$, being $R = 0.282$, $\Theta = 10^\circ$ and $D = 1$ (arbitrary units). It is worth mentioning

that the peak corresponding to the extreme minima in both graphics of Figs. 3a and 3b are located at the frequencies 0.7522 and 0.7515 which are neighbor points in a partition of the interval $\bar{\omega} \in [0.65,\ 0.95]$ constituted of 400 points. These results are within the acceptable numerical error especially considering that modeling smooth and rough surfaces implies different number of points per partition along the integration paths that limit the transverse section of the optical fiber.

A simple way to analyze the plasmonic modes is to determine the electric field intensity distribution and compare it with other modes. For example the intensity field distribution at the frequency $\bar{\omega} = 0.834$ is shown in Fig. 4 and that corresponding to the plasmonic surface mode localized at $\bar{\omega} = 0.752$ is shown in Fig. 5. It is worth noticing the contrast between the two field distributions. In particular the distribution corresponding to the plasmonic modes is highly localized in the vicinity of the interface vacuum-LHM while the field of the other mode spreads out appreciably far from this interface.

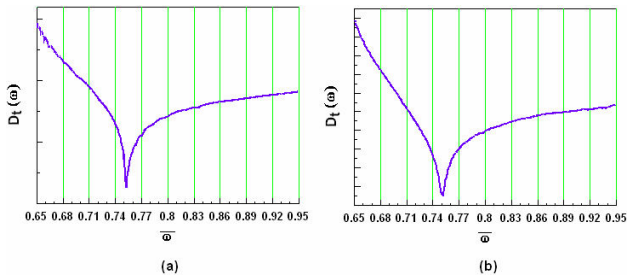

FIGURE 3. Function $D_t\,(\,\omega)$ for an optical fiber. Nucleus with a smooth surface (left), nucleus with a rough surface (right).

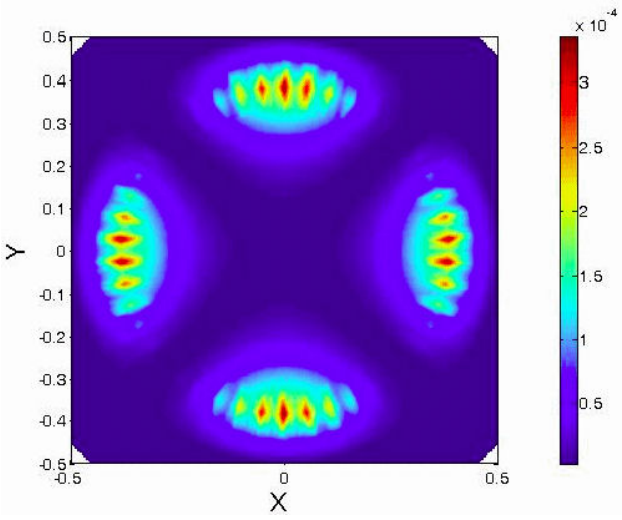

FIGURE 4. Electric field distribution for an optical fiber enclosed in a square cylinder cavity at the frequency $\bar{\omega} = 0.834$.

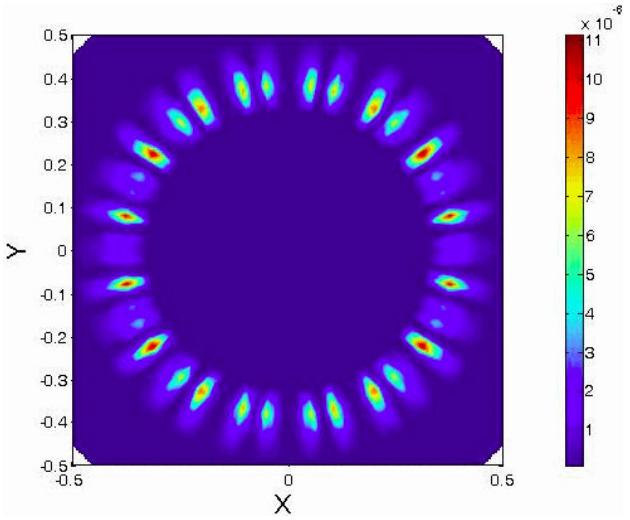

FIGURE 5. Electric field distribution for an optical fiber enclosed in a square cylinder cavity at the frequency $\bar{\omega} = 0.75$.

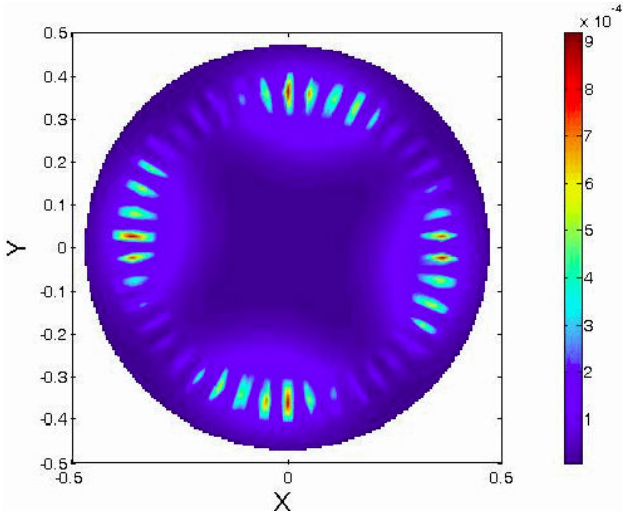

FIGURE 6. Electric field distribution for an optical fiber enclosed in a cylinder cavity at the frequency $\bar{\omega} = 0.81541$.

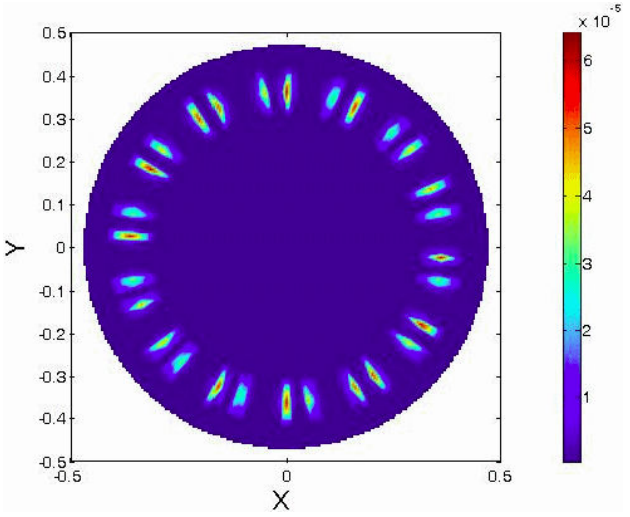

FIGURE 7. Electric field distribution for an optical fiber enclosed in a cylinder cavity at the frequency $\bar{\omega} = 0.752$.

The stability of the position of the plasmonic surface mode in the frequency space when varying the geometry can be shown more clearly by observing the intensity field distributions in Figs. 6 and 7. These fields correspond to the frequencies $\bar{\omega} = 0.81541$ and $\bar{\omega} = 0.752$ respectively, and were calculated by considering a cylindrical cavity of perfect conductor. It is worth observing that despite of these drastic geometry changes the plasmonic mode continues to be accordingly localized at the LHM-vacuum interface.

5. Conclusions

We have shown the presence of plasmonic surface modes at the surface of an optical fiber of LHM. The plasmonic modes keep perfectly localized at a constant frequency under drastic geometry changes. This fact was verified by analyzing optical fibers having smooth and random rough surfaces.

Acknowledgments

This work has been partially supported through the grant given by Subsecretaría de Educación Superior e Investigación Científica, México, Programa de Mejoramiento del Profesorado, especial Grant "Redes de Cuerpos Académicos 2004".

A. Mendoza-Suárez thanks to the CIC-UMSNH for the Grant 9.2 received for the realization of this collaboration.

1. V.A. Podolsky, *Opt. Express* **11** (2003) 735.
2. C. García-Meca, R. Ortuño, R. Salvador, A. Martínez, and J. Martí, *Opt. Express* **15** (2007) 9320.
3. V.M. Shalaev *et al.*, *Opt. Lett.* **30** (2005) 3356.
4. R. Ruppin, *J. Phys.: Condens. Matter* **16** (2004) 5991.
5. V. Kuzmiak and A.A. Maradudin, *Phys. Rev. B* **66** (2002) 045116.
6. A.A. Maradudin, E.R. Mendez, and T. Michel, *Ann. Phys.* **203** (1990) 255.
7. A. Mendoza-Suárez and E. R. Mendez, *Appl. Opt.* **36** (1997) 3521.
8. W.H. Press, B.P. Flannery, S.A. Teukolsky, and W.T. Vetterling, *Numerical Recipes the art of scientific computing* (Cambridge University Press, Cambridge, 1989).
9. Alberto Mendoza-Suárez, Ulises Ruíz-Corona, Rafael Espinosa-Luna, *Opt. Comm.* **238** (2004) 291.
10. C.D. Rabii, D.J. Gibson, and J.A. Harrington, *Appl. Opt.* **38** (1999) 4486.
11. A. Mendoza-Suárez, F. Villa-Villa, and J.A. Gaspar-Armenta, *J. Opt. Soc. Am. B* **23** (2006) 2249.
12. R. Ruppin, *Phys. Lett. A* **227** (2000) 61.